ASIA-PACIFIC SOLAR RESEARCH CONFERENCE

PEER REVIEWED
ASIA-PACIFIC
SOLAR RESEARCH CONFERENCE

Evaluating Fog Detection Using Himawari-8 Satellite Imagery and Bispectral Image Processing

Harrison I. Andrews[1], Dr Jamie M. Bright[1]

[1] *Fenner School of Environment and Society, Australian National University, Canberra 2601, Australia*

E-mail: jamie.bright@anu.edu.au

Abstract

The ability to detect fog in the solar nowcasting and forecasting space has been identified as important by Distribution Network Service Providers (DNSPs) in Australia, particularly that of Evoenergy in Canberra – Australia's foggiest city. Fog events often result in poor forecasts as the fog is often treated like cloud in satellite methodologies, as such, their motion and dissipation is erroneously accounted for. To that end, a satellite-based fog detection methodology called Bispectral Image Processing (BIP) has been explored and calibrated for use with the Himawari-8 geostationary satellite for business operational implementation. The BIP was previously detailed in literature under cloud-free cases and has not been analysed or calibrated for implementation under all sky conditions. We explore the extents and applicability of the BIP in operational simulation by calibrating its main components (i) a time-step statistic S_t, and (ii) the temperature threshold $\tau_{\Delta bT}$. Calibration and validation was carried out using fog observations from the Bureau of Meteorology ground station at Canberra Airport and Himawari-8 satellite imagery clipped to centre about the same ground station. We find relatively small differences in performance among the different S_t explored, however, the best BIP performance was offered using the 25th percentile on a 5×5 up-sampled grid with $\tau_{\Delta bT} = 5.2$K. This calibration successfully identified 68.8% of the fog events and 69.7% of the non-fog events. We find this performance unreliable but perhaps adequate because the main cause of error was due to interference of clouds, which impact the DNSPs similarly to fog.

1. Introduction

The Australian electricity distribution industry is shifting towards a decentralised network to facilitate the increasing penetration of residential photovoltaic (PV) systems. Periods of uncertain PV power output and critical power ramps caused by fog events are of concern for Distributed Network Service Providers (DNSPs). In particular, critical power ramps have been causing problems for DNSPs due to the rapid dissipation of fog. Distributed PV systems have been observed to triple their power output within 60min as the atmosphere returns to clear sky conditions (Wellby & Engerer, 2016, Fig. 1). This is a particularly challenge in Canberra – Australia's foggiest city with 46 fog days per year (Malley, et al., 2003). Additionally, the emergence of new subdivisions with 100% rooftop PV penetration is placing pressures on local DNSP Evoenergy. Evoenergy is partnered with ANU's ARENA funded PV power forecasting project. In this project, solar irradiance and PV power are estimated and forecast for the whole of Australia offering DNSPs a unique opportunity to integrate short term decision making and grid impact mitigation solutions into their regular

operations. The ARENA-project and project partner Solcast deliver state-of-the-art solar forecasts. However, fog detection and forecasting is a particular area of underperformance for many solar forecasters as fog behaves differently from clouds in that it dissipates faster and does not move as clouds do. As such, it is possible for fog to be treated as a cloud and the fog ramp is entirely missed. This is detrimental to strategic management and orchestration of such high PV penetration markets as in Canberra. To find out more about fog events in Canberra, Evoenergy asked the project to what extent fog events can be identified and forecasted using satellite imagery?

Due to the distinct properties of fog, it can be comfortably identified during day light hours using visible wavelength satellite channels (Ahn, et al., 2003). However, as fog over land generally develops at night or during pre-dawn hours, the ability to detect fog through visible images is strictly limited to daylight hours. Hunt (1973) found that clouds observed in a shortwave IR window (SIR: ~3.9 μm) had a significantly lower emissivity than in the longwave IR window (LIR: ~10.8 μm). The difference in emissivity was found to be most pronounced in clouds containing either water droplets or ice particles, such as radiation fog (Ellrod, 1994). The emissivity difference between the SIR and LIR bands is the foundation of fog identification using bispectral image processing (BIP). Eyre et al. (1984) first developed and used BIP techniques for the specific purpose of identifying fog events at night time. BIP involves deriving the brightness temperatures of both the SIR and LIR satellite scans (bT_{SIR} and bT_{LIR} respectively) and obtaining the temperature difference (ΔbT): $\Delta bT = \left| bT_{SIR} - bT_{LIR} \right|$. This relationship is not accompanied by calibration information on how to decide whether ΔbT is significantly large enough to indicate the presence of fog. A difference of 0.5K is said to represent cloud free satellite image pixels, whilst greater than 2.5K have previously been assumed to be opaque cloud (Ellrod, 1994). The issue is that there is no subjective limit set to discretise between regular cloud and fog, except that the difference is higher. For operational implementation in a live fog detection and forecasting methodology, calibration and reliability is important; thus, operational implementation within the ANU's ARENA funded project is significantly hampered.

The aim of this research is to propose and evaluate an operational satellite-based fog detection methodology that is dependable, reliable and accurate. To do this, several research objectives have been identified:

- Identify ΔbT threshold values to calibrate the simulation, enabling detection of fog and non-fog events,
- Identify appropriate statistical tests at each time-step to compare to the threshold, enabling detection,
- Test the robustness of the Himawari-8 IR windows and BIP method for fog and non-fog event detection through simulation,
- Identify limitations of the BIP method for fog and non-fog event detection,
- Propose an operational satellite-based fog detection methodology.

1.1. Contribution

There is a lack of published literature investigating the BIP's robustness and calibration. This work details a novel robustness investigation of how to operationally implement the BIP for

fog and non-fog detection. This includes an understanding of the appropriate calibration of the BIP method.

2. Data Sources

The Himawari-8 geospatial orbiting satellite is significant to the ARENA project as it provides satellite imagery data every 10-minutes with the highest spatial and temporal resolution available over Asia and the Pacific (Engerer et al., 2017). Images taken by the Himawari-8 are processed by the Australian Bureau of Meteorology (BoM) and stored on the National Computer Infrastructure (NCI) for public access. For this study, images from Band 07 (3.74 – 3.96 μm) and 13 (10.3 – 10.6 μm) at 30-minute intervals (consistent with the historical weather from the BoM) between May 2016 and May 2017 were of interest. The Himwari-8 images used in this project mimic operational implementation of a fog detection strategy.

In order to evaluate whether or not the methodology is successful, historical ground level fog observations are used for validation by corroborating the actual presence of fog when the BIP method states it as so. The Canberra Airport Weather Station (ID #070351) provided historical weather data. It was selected as it provides the most accurate recordings of fog events in Canberra due to the critical impact it can have on the aviation industry. Half hourly data was collected from May 2015 – May 2017 from the BoM. The data included many different meteorological variables, the most important being the 'Type of First Weather'. This variable provides a code that indicates the present weather conditions at the station through manual observation; one of which indicates the presence of fog ('FG').

Site #070351 is the only weather station in Canberra that records Type of First Weather. As fog is known to vary spatially (Wellby & Engerer, 2016). To limit the impact of the limited spatial extent of the fog, we analyse only those few satellite pixels in proximity to the airport. Furthermore, the Canberra Airport weather station also measures the dewpoint and ambient air temperature are recorded. This corresponding data is leveraged to apply a quality control filter describe in Section 3.

3. Methodology

Canberra Airport was isolated from within the satellite image on a $j \times j$ pixel grid. Many values of j were tested. For this research, $j = 5$ was chosen as it was assumed that an approximately 10km^2 area provided the best representation of ground data at the BOM weather station. A larger j may capture fog far from the weather station that is not locally observed, which would result in a failed test even if successfully detected.

For an image to be detected as fog during simulation, it must pass a threshold test based on the calibration information. Therefore, pixels within the spatial domain must be identifiable as fog regarding the ΔbT away from a ΔbT threshold value ($\tau_{\Delta bT}$) to enable the model to decipher between fog and non-fog time-steps. At each time-step t, we apply statistical tests (such as the mean value) on the satellite imagery to produce a time-step statistic S_t, which is then compared to a pre-defined $value\ of\ \tau_{\Delta bT}$. Thus, the simple application of the BIP model assumes the presence of fog at time-step t if $S_t > \tau_{\Delta bT}$, conversely, no fog is assumed if $S_t < \tau_{\Delta bT}$.

From Ellrod et al. (1994, fig. 1), we learn that ΔbT is largest at 200m above the cloud base height. Therefore, a simple $S_t > \tau_{\Delta bT}$ approach would also identify clouds situated over the weather station as fog. We do not wish to miscategorise cloud as fog. In order to discretise between high clouds and low fog, we take advantage of the LIR and SIR raw temperature measurements. Depending on whether a satellite image pixel contained cloud, fog or ground will influence the LIR and SIR absolute temperature reading. Clouds, being higher in the atmosphere, are naturally cooler. The surface is not too dissimilar to ambient air temperature, and fog is not too dissimilar to the ground measured dewpoint temperature. Therefore, pixels that register SIR and LIR measurements $< T_{air/dp} + 10\text{K}$ are filtered. The ambient air temperature is forecasted by numerical weather prediction models and is therefore readily available for an operational methodology.

Calibration of the threshold value $\tau_{\Delta bT}$ and time-step statistic S_t are required. For $\tau_{\Delta bT}$, a suitably low range for threshold testing was from 0K iterated every 0.1K to 30K. This provides 301 different thresholds tested. The higher the value of $\tau_{\Delta bT}$, the more strict the methodology in terms of discretising between fog and non-fog.

For S_t, there are more opportunities for how we evaluate the $j \times j$ satellite image representing the ground site at Canberra airport. For operational purposes, the ideal solution is a pixel-by-pixel analysis so that the solution is applicable upon the whole full Earth disk satellite image, however, it is difficult to state with certainty whether or not our $j \times j$ satellite image is represented by the BoM ground station due to issues such as satellite image parallax correction errors and cloud height distortion. For this reason, we consider two approaches for evaluating each image: a pixel-by-pixel approach and an all pixel summary or aggregation. Aggregation means that the whole $j \times j$ image is represented by a single S_t, such as a mean of all pixels. Both methods are implementable as an operational methodology. Due to the need for aggregate statistics, we implement an additional filter such that, if $> 70\%$ of the pixels in a time step were removed in the aforementioned ambient air temperature filter, we remove this whole time-step entirely from the validation.

The time-step statistics S_t tested in this study are:

- Mean ΔbT of the satellite image at each time-step (μ_t),
- Median ΔbT of the satellite image at each time-step (ϕ_t),
- 25th percentile of ΔbT of the satellite image at each time-step ($P_{25,t}$),
- Pixel-by-pixel comparison of each ΔbT against the threshold (ρ_t),
    - If X number of pixels corroborate the fog, fog is asserted ($\rho_{t,X=x}$)
    - X is tested at $x(1,3,5)$. $x = 5$ indicates that 20% of pixels in the image must corroborate, $x = 1$ indicates that only a single pixel must register fog to be trusted.

Our null hypothesis is that fog can be detected using the BIP methodology; the alternative being that the BIP is unsuitable with our proposed calibrations. This means that our validation becomes a classic type I and type II error analysis (Banerjee et al., 2009). There are four outcomes from our simulation at each time step: fog-present/fog-detected (success), fog-present/fog-undetected (false-negative, type II error), fog-absent/fog-detected (false-positive, type I error), and fog-absent/fog-undetected (success). Setting pass rates for type I and type II

errors(α and β values, respectively) is somewhat subjective. The relative impact of both types of error is hard to quantify, and so the importance attributed to both types through alpha and beta values is uncertain. The major instance of concern to a DNSP is a false result under clear-sky conditions; failure under clear skies from a DNSP perspective means that there will be unexpected generation or an unexpected lack of generation. Contrastingly, failure to detect under cloudy skies is less damaging as forecasts *should* have tracked the offending cloud, therefore the expected generation is low. As we cannot a-priori attribute clear-sky errors to one of the four outcomes, we adhere to standardised rates of $\alpha = 0.05$ and $\beta = 0.2$. With the inclusion of the ground temperature as a filter, we are aiming to limit a false result due to the presence of cloud, however, we have no guarantee whether this will be successful. To that end, it is also important to provide examples of a cloud interference event.

We iterate through our range of $\tau_{\Delta bT}$ recording the relative share of all outcomes when queried against S_t. Should the relative share of type I and type II errors be below α and β, respectively, then we accept the null hypothesis for that calibration. In order to decide which the best calibration is, we take the one that provides the maximum sum of success rates. A schematic of the methodology can be seen in Figure 1.

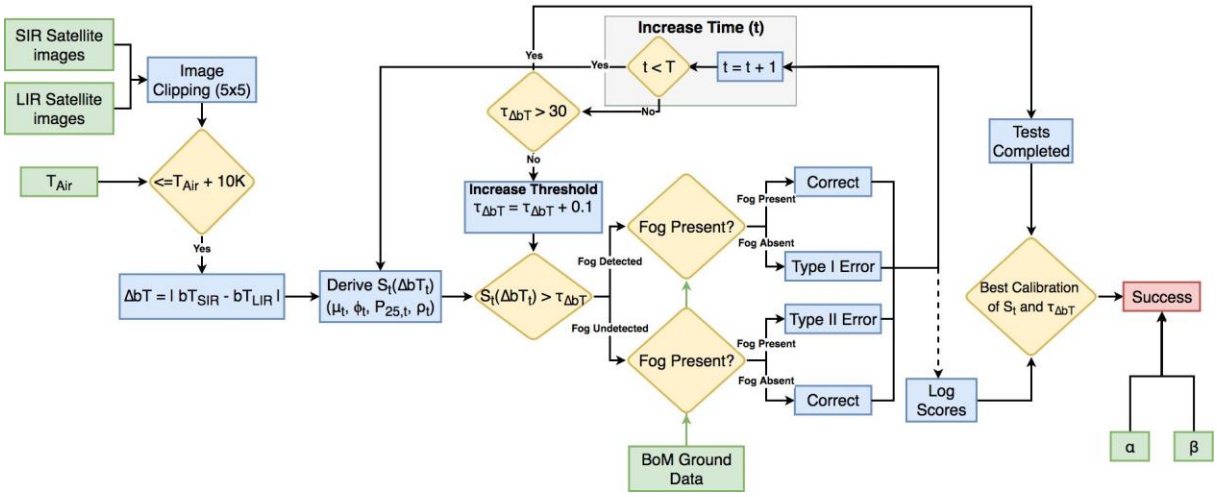

Figure 1. Methodology for assessing fog detection capability with the BIP. Green boxes represent system inputs, red boxes represent output, blue boxes represent a process and yellow diamonds represent where a decision was made by the model.

4. Results and Discussion

Figure 2 presents the results of calibration using the variety of time-step statistics and ΔbT thresholds. The plot shows the outcome of each S_t statistic versus the full range of $\tau_{\Delta bT}$. Also indicated are the pass rates for type I and type II errors which are colour coded for ease of evaluation. For successful calibration, the success rate must be above its indicated α or β.

The most notable feature is that all time-step statistics perform very similarly with only subtle differences in gradient and peak temperature threshold. The other notable outcome is the inversely proportional relationship in that, in order to mutually discretise between fog and non-fog success, one must sacrifice the accuracy of the other. Despite all the combinations of S_t and $\tau_{\Delta bT}$, there is no combination that mutually satisfies the α and β pass rates set. This

can be observed in that there is no case where both fog and non-fog detection success % are simultaneously both above the horizontal pass rate lines.

From our testing with the temperature filtering, we report that improvement is made through removal of SIR and LIR that are too cold to be ground level fog. That said, we observe very little difference to the overall success rates between the two temperature options. The dewpoint temperature (which is always less than or equal to the ambient air temperature) permits more time-steps to be analysed, which can result in subtly different success rates. Both temperature thresholds retained 157 fog observational periods and filtered 30 satellite images suspected to be cloud. The dewpoint and ambient air temperature removed 2040 and 2255 out of a total 7712 non-fog observations, suggesting that our filter is somewhat suited to discretising between cloudy and clear skies. Further testing on this filter is needed, as the brightness temperature offered by LIR and SIR are not purposed to represent the dewpoint or ambient air temperature and so there is a possibility that the filter disqualifies valid events. As the ambient temperature is more easily accessible from an operational stand point, it is recommended to use it as opposed to the dewpoint temperature.

The calibration with highest mutual success rate was when the time-step statistic $S_t = P_{25,t}$ and the ΔbT threshold was $\tau_{\Delta bT} = 5.2$K; the errors are summarised in Table 1.

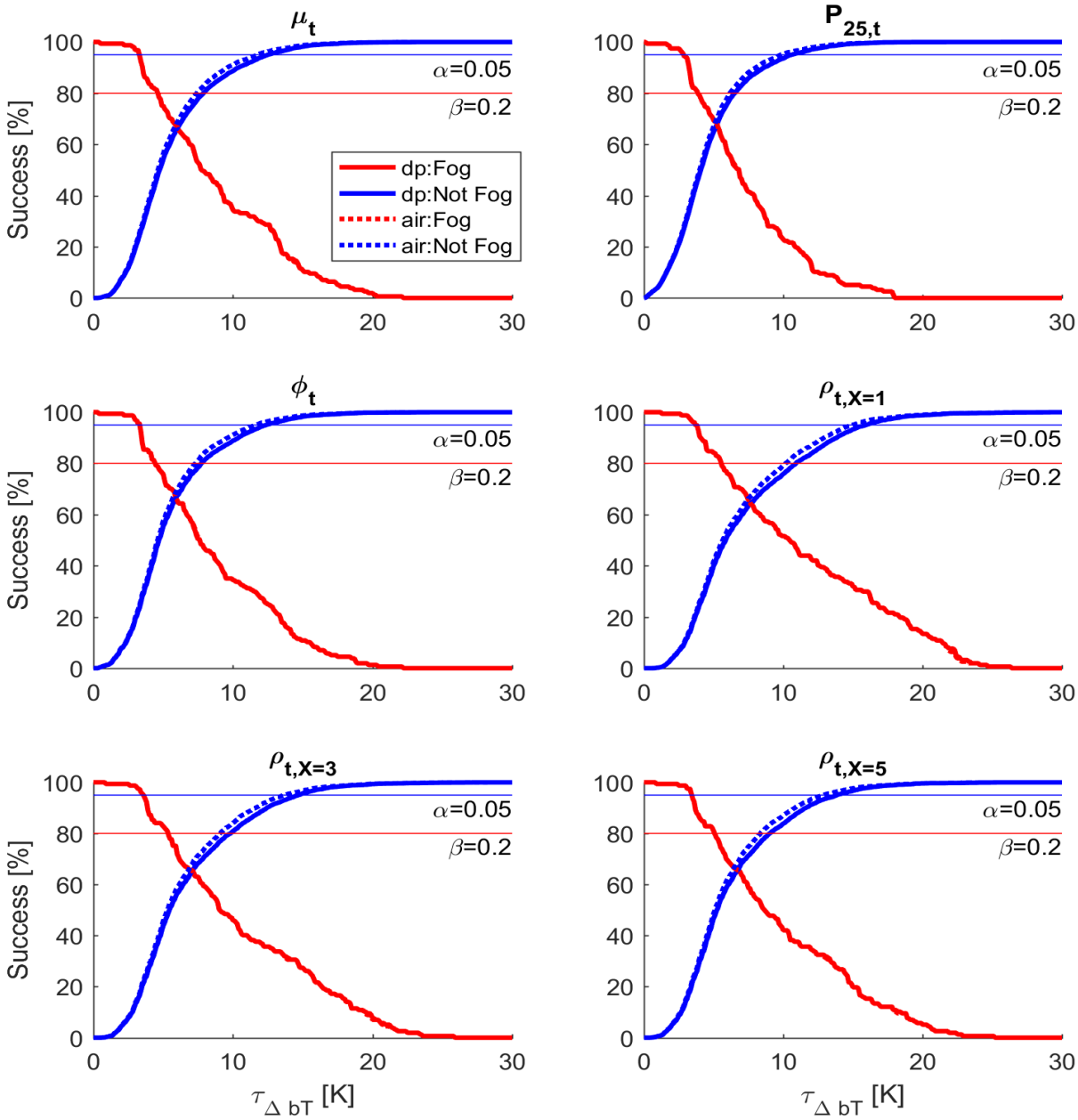

Figure 2. Operational BIP methodology success rate testing different time-step statistics S_t (mean μ_t, 25th percentile $P_{25,t}$, median ϕ_t, minimum with X=x number of corroborating pixels $\rho_{t,X=x}$) against increasing temperature thresholds $\tau_{\Delta bT}$, for both dew point (dp) and ambient air temperature approaches. Success percentage indicates what % of fog-present/fog-detected (red) and fog-absent/fog-undetected (blue) events occurred. $(1-\alpha)$ and $(1-\beta)$ values are indicated with the color-coded horizontal lines detailing acceptable type I and type II errors; the test passes if the thicker red and blue success % lines are both above their respective α and β lines. Dashed and solid lines represent identical tests except with dewpoint and ambient air temperature for filtering, respectively. Note that red-dashed line is seemingly identical to red-solid.

Table 1. Performance summary of the best calibrated BIP methodology using a $\tau_{\Delta bT} = 5.2\text{K}$, $S_t = P_{25,t}$ and LIR and SIR filtering is made using ambient air temperature. Fog-unobserved/fog-detected is type I error and fog-observed/fog-undetected is type II.

	Fog Detected	Fog Undetected
Fog Observed	108 (68.8%)	49 (31.2%)
Fog Unobserved	1653 (30.3%)	3804 (69.7%)

From Table 1, we observe the success and error rates of our calibrated BIP methodology. The best case scenario fails to satisfy our type I and type II error rate limits. Particularly for type I errors whereby the best calibration resulted in 0.303, a long way from satisfaction at $\alpha = 0.05$. Failure to satisfy our test criteria results in the rejection of the null hypothesis that fog can be detected using the BIP methodology with our defined confidence. For completeness, we report that the best calibration without the temperature filter is also $S_t = P_{25,t}$ and $\tau_{\Delta bT} = 5.2\text{K}$, however, with this calibration, we see fog observed being detected 136 (72%) times and fog unobserved being detected 4516 (58.6%) times.

Despite the rejection of the null hypothesis, it is possible that roughly 70% accuracy in overall detection is suitable for operational implementation to some extent. There are cases where the presence of cloud results in the error, in which case failure to detect or not to detect is not really an issue. The largest error is believed to be due to interference with clouds, particularly at the cloud's edge. We demonstrate this in Figure 3 where the raw and unfiltered 20×20 satellite image of both LIR and SIR are illustrated.

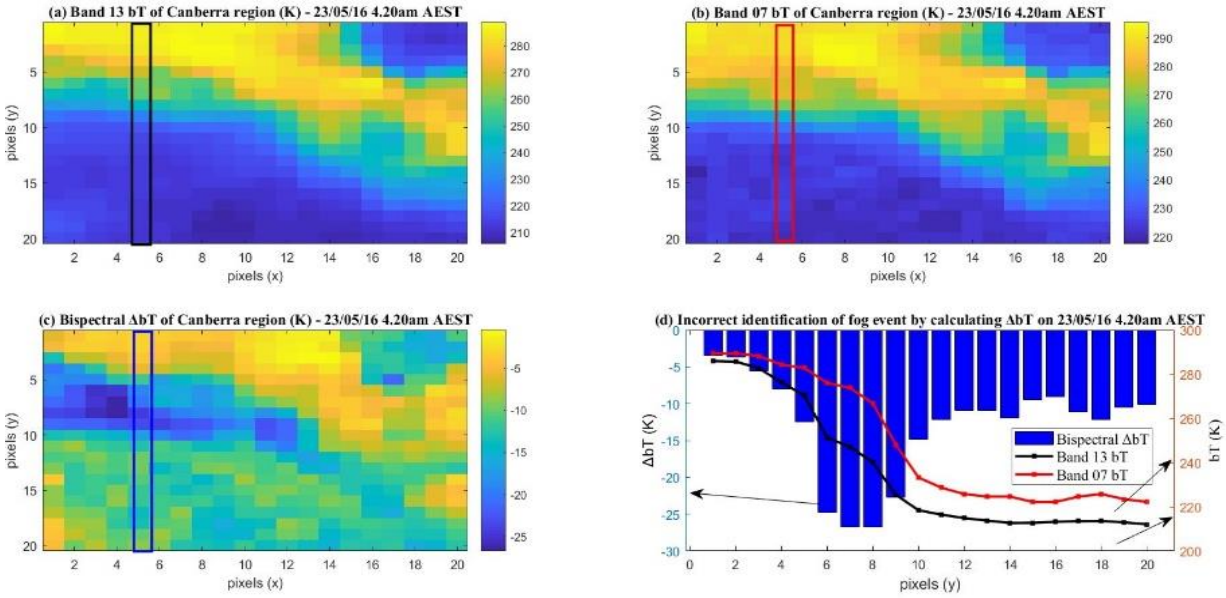

Figure 3. Type I error due to cloud edge on the 23/05/16 at 4.20am AEST with BIP. BoM observed scattered and broken clouds. Blue pixels indicate colder temperatures

(cloud), yellow indicating warmer (ground). (a) bT_{LIR}, (b) bT_{SIR}, (c) ΔbT. (d) plots of the highlighted swaths of a, b and c. Note that no absolute was taken of ΔbT in this case.

The yellow patches of the images are warmer, indicating that the satellite is measuring the earth's surface bT through a break in the clouds. At the centre of the temperature gradient between the cloud and the surface, the simulation has predicted fog to be present as ΔbT exceeds the $\tau_{\Delta bT}$ threshold, however, this is only the cloud edge and no ground fog was observed.

This illustrates the importance of cloud filtering using ground estimated temperatures. To explore the influence that the proposed temperature filtering ($T_{air/dp} + 10$K) has on ΔbT_{LIR} and ΔbT_{SIR}, the filter is illustrated in Figure 4. We are confident in discretising pixels that are significantly below the filter as cloud, however, it is more difficult to discritise close to the filter. It is quite certain that the left sided fog temperatures that are as low as 200K must be cloud obscuring the ground during a fog event. We believe the filter to be suitable.

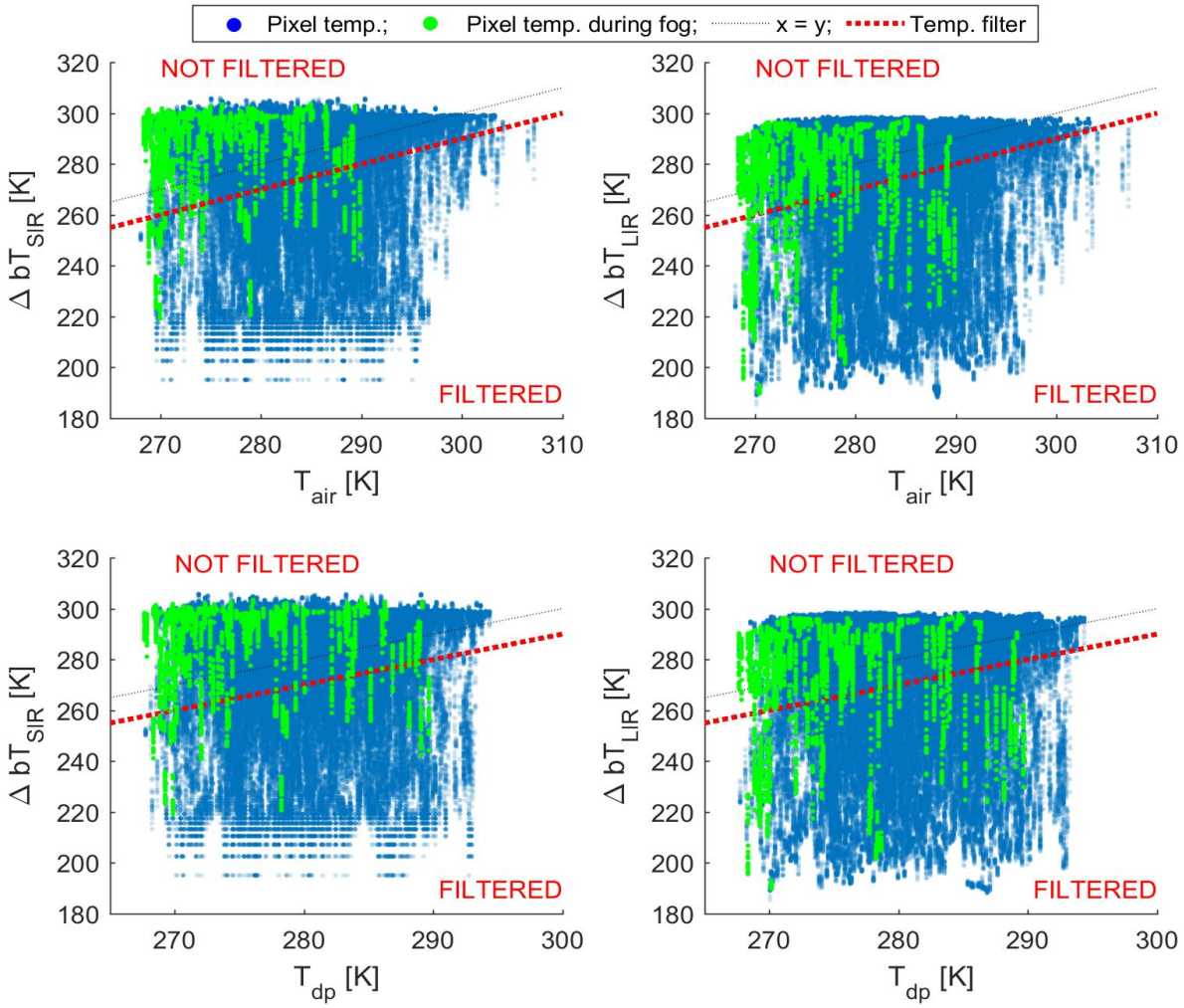

Figure 4. Scatter plots of the Himawari-8 SIR and LIR brightness temperatures against the ground measured ambient air and dewpoint temperatures from the BoM. The red dashed line indicates the filter that was applied in this study. Green dots represent the

full $j \times j$ set of pixels during a BoM observation of fog. Measurements above the red line are not filtered during our quality control routine, those below are.

There are several improvements that can be done to both the analysis and implementation of the fog detection model. Firstly, the removal of time-steps where cloud is known to be present above recorded instances of fog would remove unfair assessment of the BIP. When the cloud is covering fog, the impacts of fog become negligible. The fact that the BIP is not advertised as a methodology for analysis under clouds means that the inclusion of these time-steps is not ideal for suitable evaluation; thus, deeper analysis of the model would be enabled. The inclusion of the ground temperature in order to filter SIR and LIR was expected to handle the issue of cloud presence, however, it fails to in a few cases. There are clear occasions where cloud edges are misjudged as fog events due to significantly large ΔbT values that have passed through the filter. There is the potential to integrate cloud motion vector projection from the LIR channel, which will identify the presence of water in cloud form at night time. Using pre-known cloud motion vectors, it would be possible to attribute cloud presence a-priori, and ultimately discount those pixels from fog analysis.

5. Conclusion

The bispectral image processing (BIP) for fog and non-fog event detection using the Himawari-8 satellite was evaluated. Previously, the BIP has only been demonstrated to work under clear-skies with no definition of calibration for operational application. This research paper has applied the BIP method with realisable methodologies that could be applied into the ARENA-funded solar forecasting methodology. We evaluated the BIP method through simulation and validation against ground data in Canberra, Australia. Our implementation was simple such that a statistic (mean, median etc.) derived at each time-step from the satellite data (S_t) was directly compared to an increasing range of temperature threshold values ($\tau_{\Delta bT}$). Satisfaction of this comparison resulted in the assertion of fog. We report that the best calibration of the BIP methodology was a combination of $\tau_{\Delta bT} = 5.2$K and $S_t = P_{25,t}$, which is the 25th percentile at a 5×5 assimilated satellite image. Despite the best performance at this calibration, the methodology only successfully identified 68.8% of fog events and 69.7% of non-fog events. This results in considerable type I and type II errors, far greater than permissible rates of α and β required for a reliable methodology. Ultimately, with the calibrations analysed, we must reject the null hypothesis of using BIP methodology for fog detection at this time. That said, the requirement and reliability placed on the fog events is not overly severe, and so a roughly 70% success rate may be adequate at this time lending argument to reduced α and β. Particularly as failure to detect cloud is primarily due to cloud presence, as such the impact on PV power and grid integration is much the same. Therefore, the BIP is perhaps suitable in this instance for DNSP usage, though not for Aviation.

This preliminary analysis confirmed that the detection of fog events was often made impossible due to the presence of cloud and cloud edges resulting in excessive occurrences of type I and II errors. More input parameters are required to accompany the BIP in order to inform which pixels of the image are suitable to perform the BIP on. Future improvements using a-priori cloud motion vectors could improve the discretisation of when and where to implement the BIP such that there can be statistical confidence in the results.

Acknowledgements

Jamie M. Bright was funded by the Australian Renewable Energy Agency (ARENA, Research and Development Programme Funding G00854).

References

Ahn, M., Sohn, E. and Hwang, B., 2003, 'A New Algorithm for Sea Fog/Stratus Detection Using GMS-5 IR Data', *Advances in Atmospheric Sciences*, 20, p899-913.

Banerjee, A., Chitnis, U. B., Jadhav, S. L., Bhawalkar, J. S., and Chaudhury, S, 2009, 'Hypothesis testing, type I and type II errors', *Ind Psychiatry J.*, 18, p127-131.

Ellrod, G., 1994, 'Advances in the Detection and Analysis of Fog at Night Using GOES Multispectral Infrared Imagery', *Weather and Forecasting*, 10, p606-619.

Engerer, N., Bright, J. and Killinger, S., 2017, 'Himawari-8 enabled real-time distributed PV simulations for distribution networks', *IEEE Photovoltaic Specialist Conference, PVSC44, 25th-30th June 2017, Washington DC, USA.*

Eyre, J., Brownscombe, J. and Allam, R., 1984, 'Detection of fog at night using Advanced Resolution Radiometer (AVHRR) imagery', *Meteorology Magazine*, 113, p266-271.

Hunt, G., 1973, 'Radiative properties of terrestrial clouds at visible and infrared thermal window wavelengths', *Meteorology Society*, 99, p346-369.

Malley, S., Miao, Y., Davis, C., and Forrest, A., 2003, 'A study of fog statistics and forecasting aids at Canberra Airport', Melbourne: Australian Bureau of Meteorology.

Wellby, S. and Engerer, N., 2016, 'Categorising the Meteorological Origins of Critical Ramp Events in Collective Photovoltaic Array Output', *Journal of Applied Meteorology and Climatology*, 55, p1323-1344.